An experimental study on explosive boiling of superheated droplets in vacuum spray flash evaporation

Wenzhong Gao[1], Jiahao Zhang[1], Xuan Yang[1] ,Guangming Chen[2], Dawei Wu[3]

(1. Merchant Marine College, Shanghai Maritime University, Shanghai, 201306, China; 2. Zhejiang University, Hangzhou, China; 3.School of Engineering, Newcastle University, Newcastle upon Tyne, NE1 7RU, United Kingdom)

Abstract: Spray flash evaporation is an effective desalination method, which increases specific surface area of salty water by liquid atomization, thereby improving desalination performance and maximising low-grade heat source utilization. During evaporation, explosive boiling phenomenon occurs inside superheated droplets on a heated surface. In order to understand the mechanism of explosive boiling, spray flash evaporation of distilled water and 3.5wt% salty water in a high vacuum vessel was observed visually. Meanwhile, a parametric study was carried out to scrutinize the impacts of the variation of ambient pressure, heat flux, and surface superheat degree. The experiment data indicates that nucleate site is located in the upper layer of a droplet due to internal superheated liquid and Marangoni convection. In different operating conditions, bubble fragmentation process or crown fragmentation process happens at nucleate site. The fragmentation time of pure water, which is mainly influenced by heat flux and surface superheat degree, shrinks with higher heat flux and higher surface superheat degree. The fragmentation time of 3.5wt% salty water decreases with ambient pressure drops and superheat degree increments.

Keywords: desalination; spray flash evaporation; explosive boiling; fragmentation time; Marangoni convection

Nomenclature

Ambient pressure（Pa）	p	Surface tension（N/m）	σ
Power of electric heating rods（W）	P	Liquid density（kg/m³）	ρ
Surface superheat degree（℃）	T_Δ	Droplet fragmentation time（ms）	τ
Heat flux（W/cm^2）	q	Droplet fragmentation count	N
Cooling temperature（℃）	T_C	Surface temperature（℃）	T_w
Boiling point（℃）	T_0		

1. Introduction

Desalination processes could be classified into two categories [1]: thermal desalination processes and membrane-based processes. As one of the key desalination processes, thermal desalination processes include multi-stage flash (MSF), low temperature multi-effect distillation (LT-MED), vapor compression (VC), solar still desalination (SD) and humidification-dehumidification （HDH）[2]. MSF evaporation is one of the most widely used desalination methods due to its multistage utilization of latent heat and large unit capacity. MSF could also deal with salty water in high concentration (up to 70000 mg/L) [3]. However, single stage separation rate of MSF evaporation remains low (0.8%-1.4%), since the latent heat of flash evaporation is supplied by the sensible heat of seawater [4].

As one of the thermal desalination processes, spray flash evaporation atomizes liquid to increase specific surface area, thereby enhancing separation rate. Moreover, spray flash evaporation requires small temperature difference, so it shows a great potential in utilizing low-grade heat source [5][6].

In 1981, Miyatake et al. [7][8] proposed spray flash evaporation technology. The distilled water was injected into the flash chamber through circular tube nozzle with the inlet temperature of 40-80℃. They concluded that the evaporation performance

and the separation rate of the spray flash evaporation could be extremely higher than those of conventional MSF evaporation. After that, the influence of the number of bubble nuclei was studied to further improve the evaporation performance [9]. The bubble nuclei were created through electrolysis at the nozzle inlet. The experiment results led to the conclusion that artificial nucleation could provide higher evaporation performance, thereby reducing non-equilibrium loss. Mutair et al. [10][11], Araghi et al. [12], Cheng et al. [13][14] carried on experiments and simulation studies on influencing factors which affect the flash evaporation. The influencing factors include solution spray flow, average size of liquid droplets, spray flow temperature, superheat degree, the diameter of the nozzle and so on. Moreover, Balaji et al. [15] investigated the effects of different spout nozzle geometries with different heights on flash evaporation rate and non-equilibrium temperature difference. The experiment results were compared to the values calculated by empirical correlations from the work of Miyatake et al. [16] and Al-Juwayhel et al. [17]. The results showed that the actual flash efficiency would fall short of the predicted value if the duration of flash evaporation is insufficient.

In a pilot application, Mutair et al. [18] constructed a small vacuum flash desalination plant in 2010. The maximum production of distilled water was up to 15.2 tons/day. In 2016, Hamawand et al. [19] proposed a novel vacuum flash desalination system with the aid of solar energy. To increase the separation rate, the inlet water was preheated using the waste heat of the vacuum pump and the solar energy. The productivity of the desalination was about 15kg/m^2/day. Furthermore, an energy saving desalination system was created by Miyatake et al in 2001 [16] to combine phase-change energy storage and spray flash evaporation. With the energy storage, low-grade heat sources such as solar energy and industrial waste heat were stored to preheat the salty water, which achieves desalination performance improvement.

To further improve separation rate and make full use of low-grade heat source,

Wenzhong Gao [4][20] developed a novel spray flash vacuum evaporator through using heat pipes to reheat seawater. The influence of nozzle height, solution spray flow, spray flow temperature and heat source temperature was analyzed. The results indicated that the separation rate of flash evaporation is significantly higher than that of conventional single stage flash evaporation due to the secondary heat transmission of the heat pipes. The maximum separation rate was up to 65%.

It should be noted that when subcooled mist droplets hit heated surface, some of diluted solution forms liquid film or large droplets rather than evaporating completely. It is noticeable that the explosive boiling phenomena occur inside the large droplets or liquid film [21]. This suggests that after hitting the heat pipes, the solution is superheated rapidly and transits into the metastable state.

About this phenomenon, Owen et al. [26] presented an approach to observe the heterogeneous flashing inside solution droplets under various superheating temperatures. With rapid depressurization, droplets under the saturation temperature with the diameter between 1 and 3 mm were superheated. The droplets would not evaporate until superheat degree reaches 5℃. For superheat temperature between 5~18℃, internal boiling could be found inside droplets. When superheat temperature is above 18℃, the droplets experience explosive boiling. Moreover, the droplet kinematics has an impact on the heat and mass transfer of droplets. Through experiment, Liu et al. [27] proposed that droplet movement enhances flash evaporation performance at the early stage of depressurization. Lu et al. [28] investigated the phase change characteristics of the droplets in the nucleate boiling period. The results showed that the confine boiling mechanisms could be affected by Marangoni convention, and the heat transfer rate decreases while the bubbles are growing and merging.Volkov et al. [29][30] studied temperature and velocity inside the droplet and on its surface by analyzing the droplets in space and heated surface,and revealed the effect of convective heat transfer on the external and internal

droplets on evaporation.

Explosive boiling during vacuum flash evaporation shows its great particularity because of the heating of the supercooled droplets. The phenomena of droplet explosive boiling and its associating mechanisms are still unknown, which motivates this work. The vacuum explosive boiling characteristics inside the droplets of pure water and 3.5wt% NaCl solution are studied in the experiments, with the aid of a high-speed image capture device. The heat pipes are simulated by electric heating rods. The influence of heat flux, ambient pressure, and surface superheat degree are revealed.

2. The experimental system and testing methodologies

2.1. Experimental system introduction

As shown in Fig. 1, the experiment devices include the flash chamber, the condensing chamber, the concentrated solution tank, the dilute solution tank, the vacuum pump, the DC power supply, the image acquisition system and the data collection system. The flash chamber is composed of two blind plates and borosilicate glass tube with a diameter of 180mm and 10mm thickness. The blind plates are made of stainless steel with a volume of 316L. For the airtightness of the flash chamber, the O rings are filled in the gaps between the blind plates and the glass tube.

The condensation chamber, the vacuum pump, and the Agilent data logger are connected to the upper blind plate. The steam generated during the desalination is cooled by the condenser which consists of cooling coil and condensing chamber. The vacuum pump vents the non-condensable gas periodically.

The under blind plate has 3 electric heating rods and a liquid outlet installed. The electric heating rods are powered by the DC power supply with the unit power output of 100w. The concentrated solution tank is connected to the liquid output to recycle

the salty water.

2.2. The data acquisition system

The data acquisition system is made up of the image acquisition system and the data collection system. The performance parameters of the measurement devices are shown in Table 1. As shown in Fig. 2, the thermocouples, which are fixed with high temperature tape, are distributed evenly on the one side of the electric heating rods. The values of absolute pressure and temperature are collected by the Agilent data logger.

The image acquisition system includes a high-speed camera (AOS X-PRI, Switzerland) and a 150w Halogen cold light source. The maximum photo capture rate is 1,000 frames with a resolution of 800×600. The duration of a single video is 5.5s. The time zero of 0ms is set 1ms ahead the explosive boiling occurs. The size of droplets is measured by AOS Imaging Studio.

2.3. Experiment methodologies

First, the data collection system was started to monitor the values of temperature and pressure. The focal length of high speed camera was adjusted to have a high resolution on the objects. Then, the pressure was adjusted to meet the required value of corresponding operating condition by the vacuum pump. When all the parameters were stable, the vacuum valve between the flash chamber and diluted solution tank opened. The solution was atomized into a large number of mist droplets by pressure difference in the centrifugal nozzle. Due to the instantaneous depressurization, the mist droplets flashed intensively, which led to the sharp descending temperature of the remaining mist droplets. During the droplet movement, the explosive boiling phenomena would occur after the subcooled droplets hit the heated surface. After this, the remaining liquids formed into the falling film. To keep the pressure stable, the steam generated during the evaporation process was condensed in the condensing

chamber. The concentrated solution was recycled in the concentrated solution tank through the liquid outlet.

2.4. Working conditions

Experimental conditions are shown in Table 2.Based on the background of low temperature waste heat seawater desalination system,the temperature of heating surface ranges between 40-80 degrees to simulate low-grade heat source,the pressure of working environment ranges from 3kpa to 10kpa due to the saturation pressure of pure water at room temperature is 3kpa.In all conditions, the nozzle height, spray flow rate and condenser temperature keep as the constants, i.e. 80mm, 200ml/min and 12℃, respectively. The ambient temperature is about 30 ℃. The voltage (V) and current (I) could be acquired by DC power supply. The average heat flux q is evaluated based on equation (1)

$$q_w = \frac{Q}{A} = \frac{VI}{\pi DL} \tag{1}$$

where D and L are the cross-sectional diameter and length of the heating rod.

The superheat temperature T_Δ is evaluated by equation (2)

$$T_\Delta = T_w - T_0 \tag{2}$$

where T_w is the temperature of the heated surface, and T_0 is the corresponding boiling point of the vacuum degree.

The boiling point of pure water under different vacuum degree is acquired by consulting the component property data manual. The boiling point of 3.5wt% salty water under different vacuum degree is acquired by Thermophysical properties of seawater collected by MIT. The correlations developed in the library, the original data sources, the validity ranges, and the uncertainty in each property function are proposed by Nayar [31] and Mostafa [32].

3. Results and discussion

3.1. Classic fragmentation processes

(1) Classic fragmentation processes of pure water

Fig. 3 shows the bubble fragmentation processes of pure water in condition 1. The droplets start to absorb heat after depositing on the surface. It could be found that a white foamed area occurs on the upper layer of the droplet at 1 ms. Then, a tiny nucleate bubble immediately generates at the foamed area. It continues expanding until the size of the bubble is large enough (12.7mm). As the internal pressure of the bubble is greater than the surface tension of the liquid film, the bubble bursts and the liquid film collapses. Some of the water splashes while the other still sticks to the heating surface.

Besides the bubble fragmentation processes, the crown fragmentation processes could be found during the experiment, following the increase of heat flux and the increase of surface superheat temperature. As shown in Fig. 4, the initial phenomenon of the crown fragmentation processes is similar to that of the bubble fragmentation processes. The white foamed area appears on the upper layer of the droplet. At 2 ms, the internal liquid of the droplet vaporizes instantly. The instantaneous steam production is much more than that of the bubble fragmentation processes, thereby restraining the bubble fragmentation process. Then, a steam column ejects from the foamed area and forms into the crown liquid film resembling an inverted cone at 5 ms. At 6ms, the whole liquid film begins collapsing under the synergy of surface tension and absolute pressure difference. It should be noted that a mass of tiny secondary atomization droplets splashes because of the fragmentation of the liquid film, which is caused by the unbalanced forces of the liquid film.

(2) Classic fragmentation processes of salty water

Fig. 5 depicts the bubble fragmentation processes of 3.5wt% salty water in

condition 6. As similar to the bubble fragmentation processes of pure water, the internal liquid of the droplet vaporizes sharply when the superheated salty water could no longer keep the metastability. Then, a bubble occurs at the nucleation site. The bubble has been growing continually until it bursts in the joint effect of the imbalanced pressure and the surface tension. It is noteworthy that the bubble birth time and the bubble fragmentation time (the time between nucleation site occurs on the upper aqueous layer and the main body of droplet bursts completely) of salty water are usually shorter than that of pure water in the same experimental conditions.

Fig. 6 shows the crown fragmentation process of 3.5wt% salty water in condition 7. At 1 ms, there occurs the white foamed area on the droplet surface before the explosive boiling. Unlike pure water, there is no white steam column ejecting from the foamed area. The inverted cone liquid film occurs directly while the internal liquid of salty droplet vaporizes rapidly. The collapse processes of the liquid film are similar to that of the pure water.

(3) Evaporation process comparison between atmospheric pressure and vacuum

As can be seen from above description,the overall evaporation process of the droplets under vacuum is the ms level and the evaporation process is intense.While under atmospheric pressure [28][33],the whole evaporation process is three orders of magnitude larger than that under vacuum,the evaporation process is also relatively mild.Meanwhile,bubble growth and breaking rate and droplets break rate is totally different,it is much bigger under vacuum. The shorter bubble growth and breakage cycle of binary mixture solution shows its faster evaporation rate,however,when it comes to atmospheric pressure [33],the value of pure water is larger than binary mixture solution.

3.2. Mechanism analysis of droplet explosive boiling

Usually, when the droplet is heated at atmospheric pressure, several nucleate

bubbles grow at the solid-liquid surface between the droplets and the heated surface [28]. However, the vacuum explosive boiling of the droplets is totally different. As shown in Fig. 3 - Fig. 6, the explosive boiling phenomena happen immediately after the single nucleate site occurs at the upper layer of the droplet. Furthermore, at the same ambient pressure, the explosive boiling phenomenon of 3.5wt% salty water is far more violent than that of pure water even with the greater surface tension. It indicates that the behavior of droplet explosive boiling in a vacuum is influenced by internal superheated liquid and Marangoni convection.

The Marangoni convection is mainly affected by temperature gradient and concentration gradient [33][35]. As shown in Fig. 7, water near the heated surface is heated during the vaporization process. While the liquid at the rim around the solid-liquid surface is vaporizing, the internal liquid moves to the rim spontaneously to make up for the loss. Due to the non-uniform distribution of the temperature field[28], the liquid of the lower layer is much hotter, which causing the lower surface tension. Therefore, the pull from the upper aqueous layer is stronger than that of the lower layer. The surface tension gradient caused by temperature difference leads to the origination of Marangoni convection. The convection, in turn, drives the hot water to the upper layer (the cold region) along the liquid-gas interface, thus promoting the liquid update on the droplet surface.

Moreover, in a high vacuum, when the droplets deposit on the heated surface, the liquid of the lower aqueous layer would be overheated in a very short time. As a result, the superheated liquid would be transited into the metastable state. However, the temperature of the upper layer remains low because heat transfer takes time[36]. Meanwhile, the superheated liquid flow to the upper layer driven by the Marangoni convection. When the superheated liquid contacts the colder one, it could not preserve the metastable state. Finally, a nucleate bubble is generated suddenly and spontaneously. The explosive boiling is triggered [21].

Compared with pure water, the explosive boiling of 3.5wt% salty water is under the action of both the Marangoni thermal convection and the Marangoni convection caused by concentration gradient. This makes not only the stronger liquid update on the droplet surface, but also the more unbalanced forces. For this reason, under the same condition, the Marangoni convection of salty water is much stronger, thereby causing the greater explosive boiling [35].

3.3. Influence of experiment parameters

(1) Influence of ambient pressure

Fig. 8 summarizes the distribution of the fragmentation time of water droplets in condition 5 with the absolute pressure of 3~10 kpa. As it can be seen, the distribution of the fragmentation time is similar to normal distribution. The peak values of the data in the range of 4-10 ms remain unchanged. This illustrates the ambient pressure has limited influence on the fragmentation time. Meanwhile, the droplet fragmentation count (the count of droplet fragmentation in a single video with the duration of 5.5s) increases with the decreasing pressure. The counts of the droplet fragmentation at 7 ms are 27, 22, 20, 3respectively for 3, 5, 7.5, 10 kpa pressure. This is because the Marangoni convection of pure water is only influenced by temperature gradient, which is slightly affected by the pressure variation. However, the boiling point of water decreases due to the lower ambient pressure. Therefore, the heated liquid becomes more easily to be superheated, causing the higher fragmentation count.

Fig. 9 shows the distribution of fragmentation time of 3.5wt% salty water in condition 6. The range of absolute pressure is from 5 to 10 kpa. Like pure water, the distribution of fragmentation time is similar to normal distribution. The fragmentation time is mainly distributed in 4-10 ms. However, the peak value shifted to left when the lower absolute pressure applies. For the absolute pressure of 10, 7.5 and 5 kpa, the peak values are 11, 7, 5 ms and the count of fragmentation time are 5, 23, 40. With lower pressure, the fragmentation time is shortened while the fragmentation count

increases. This suggests that the ambient pressure is a key parameter of explosive boiling of salty water. The reason is that the concentration of the solid-liquid surface increases while the liquid at the rim is vaporizing. The enhanced Marangoni convection, which is influenced by both temperature gradient and concentration gradient, intensifies the process of explosive boiling.

(2) Influence of heat flux

Fig.10-12 shows the effect of heat flux on the explosive boiling in condition 7, 8, 9 and10 with the heat flux range of 0.5~1.5w/cm^2. As shown in Fig.10 and Fig. 11, the fragmentation time of pure water is distributed as the similar normal distribution. As shown in Fig. 10, when the heat flux is 0.5w/cm^2 with the pressure of 5 kpa, the peak value is 11ms. Meanwhile, the fragmentation time is widely distributed with the fluctuating fragmentation count. With the increasing heat flux, the fragmentation time decreases gradually and the peak value shift to left. The fragmentation count increases enormously. For instance, the fragmentation time is mainly distributed in 5-10 ms with the heat flux of 1.5w/cm^2. The peak value is decreased to 6ms while the fragmentation count increases greatly. The similar phenomena occur with the pressure of 7.5 kpa, as shown in Fig. 11. This is because the increasing heat flux enhances the non-uniform distribution of temperature, thereby strengthening the Marangoni convection. Thus, the fragmentation time decreases and the fragmentation count increases.

Different from the pure water, the increasing heat flux has almost no influence on the distribution of the droplet fragmentation time of 3.5wt% salty water, as shown in Fig. 12. For the ambient pressure of 5 and 7.5 kpa, the distribution of fragmentation time is mainly 3-8 ms and 6-10 ms with the peak value of 5 and 7 ms, respectively. However, the fragmentation count increases with the increasing heat flux. Conclusion can be made that the Marangoni convection is also under the action of concentration gradient for salty water, which makes the disturbance big enough.

Therefore, the increasing heat flux has limited effect on the fragmentation time.

(3) Influence of surface superheat degree

Fig. 13 shows the distribution of fragmentation time of pure water with the absolute pressure of 5 kpa in condition 11. The explosive boiling phenomena occur when the surface superheat of pure water rises to 10℃. The fragmentation time decreases and tends to be stable with the increasing of the surface superheat degree. Due to the larger temperature difference of the solid-liquid surface, the temperature of the lower aqueous layer is higher. Therefore, the disturbance inside the droplets enhanced due to the Marangoni convection, causing the greater explosive boiling and decreasing fragmentation time.

Fig. 14 shows the effect of surface superheat degree on fragmentation time of 3.5wt% salty water in condition 12 and 14. The absolute pressure are 5, 7.5 kpa, respectively. Like pure water, the fragmentation time of salty water decreases with the increasing surface superheat degree. It should be noted that the gap of the fragmentation time under different heat flux is narrowing down with superheat degree. For instance, the gap of the droplet fragmentation time with 0.5w/cm^2 and 1.5w/cm^2 decreases with the increasing surface superheat degree. When the surface superheat temperature rises to 40℃, the gap is almost disappeared. This illustrates that the effect of heat flux is weakened because of the enhanced Marangoni convection. The reason is that the concentration gradient increases with the increasing surface superheat, which promotes the Marangoni convection.

4. Conclusion

To study the heat and mass transfer mechanism of the explosive boiling inside the superheated droplets during the spray flash evaporation, the phenomena of spray flash evaporation were observed with visualization device. The temperature and pressure changes were obtained in the experiment. The influence factors and their

effects on pure water and 3.5wt% salty water were analyzed. The influence factors include ambient pressure, heat flux and surface superheat degree. The main conclusions are summarized as follows:

(1) In vacuum conditions, both the bubble fragmentation processes and the crown fragmentation processes occur inside the droplets of pure water and 3.5wt% salty water. During the explosive boiling processes, the bubble or crown film are generated at the nucleate site located on the upper layer of the droplets.

(2) The behavior of explosive boiling of droplets in vacuum is mainly influenced by internal superheated liquid and Marangoni convection. Ambient pressure, heat flux and superheat degree are the main influence factors. Moreover, the explosive boiling of 3.5wt% salty water is much greater than that of pure water due to the Marangoni thermal convection and Marangoni convection caused by the concentration gradient.

(3) The fragmentation time of pure water is mainly affected by heat flux and surface superheat degree. The ambient pressure has limited influence on the fragmentation time. The fragmentation time will reduce as the heat flux increases and surface superheat degree increases. Moreover, the fragmentation count increases with the decrease of the ambient pressure and the increasing of the surface superheat degree.

(4) The fragmentation time of 3.5wt% salty water is mainly controlled by ambient pressure and surface superheat degree, which has limited influence from heat flux. It is shortened with the decrease of the ambient pressure and the increase of the surface superheat degree. The fragmentation count increases with higher heat flux and lower ambient pressure.

Acknowledgments

The research work described in this paper was supported by the National Natural Science Foundation of China (Grant No.51106094) as well as Natural Science Foundation of Shanghai (Grant No. 16ZR1414700). Their supports are gratefully acknowledged by the research team.

References

[1] Ahmed Alkaisi, Ruth Mossad, Ahmad Sharifian-Barforoush, A Review of the Water Desalination Systems Integrated with Renewable Energy, In Energy Procedia, Volume 110, 2017, Pages 268-274, ISSN 1876-6102.

[2] Alkaisi, Ahmed, Ruth Mossad, and Ahmad Sharifian-Barforoush. "A Review of the Water Desalination Systems Integrated with Renewable Energy." *Energy Procedia* 110 (2017): 268-274.

[3] Chandrashekara M, Avadhesh Yadav, Water desalination system using solar heat: A review, In Renewable and Sustainable Energy Reviews, Volume 67, 2017, Pages 1308-1330, ISSN 1364-0321.

[4] Gao, Wenzhong, et al. "Experimental study on water separation process in a novel spray flash vacuum evaporator with heat-pipe." *Desalination* 386 (2016): 39-47.

[5] Chen Q, Ja M K, Li Y, et al. Experimental and mathematical study of the spray flash evaporation phenomena[J]. Applied Thermal Engineering, 2017.

[6] Ikegami Y, Sasaki H, Gouda T, et al. Experimental study on a spray flash desalination (influence of the direction of injection)[J]. Desalination, 2006, 194(1-3): 81-89.

[7] Miyatake O, Tomimura T, Ide Y, et al. An experimental study of spray flash evaporation[J]. Desalination, 1981, 36(2): 113-128.

[8] O. Miyatake, T. Tomimura, Y. Ide, M. Yuda, T. Fujii, Effect of liquid temperature on spray flash evaporation, Desalination 37 (3) (1981) 351–366.

[9] Miyatake O, Tomimura T, Ide Y. Enhancement of Spray Flash Evaporation by Means of the Injection of Bubble Nuclei. ASME. J. Sol. Energy Eng. 1985;107(2):176-182.

[10] Sami Mutair, Yasuyuki Ikegami, On the evaporation of superheated water drops formed by flashing of liquid jets, In International Journal of Thermal Sciences, Volume 57, 2012, Pages 37-44, ISSN 1290-0729

[11] Mutair, S., & Ikegami, Y. (2012). On the evaporation of superheated water drops formed by flashing of liquid jets. International Journal of Thermal Sciences, 57, 37-44.

[12] A. Hosseini Araghi, M. Khiadani, M.H. Sadafi, K. Hooman, A numerical model and experimental verification for analysing a new vacuum spray flash desalinator utilising low grade energy, In Desalination, Volume 413, 2017, Pages 109-118, ISSN 0011-9164.

[13] Cheng, W.-L., Peng, Y.-H., Chen, H., Hu, L., & Hu, H.-P. (2016). Experimental investigation on the heat transfer characteristics of vacuum spray flash evaporation cooling. International Journal of Heat and Mass Transfer, 102, 233-240.

[14] Cheng, W.-l., Chen, H., Hu, L., & Zhang, W.-w. (2015). Effect of droplet flash evaporation on vacuum flash evaporation cooling: Modeling. International Journal of Heat and Mass Transfer, 84, 149-157. doi: 10.1016/j.ijheatmasstransfer.2014.12.078

[15] Balaji, D. (2016). Experimental study on the effect of feed water nozzles on non-equilibrium temperature difference and flash evaporation in a single-stage evaporator and an investigation of effect of process parameters on the liquid flashing in a LTTD desalination process. Desalination and Water Treatment, 57(56), 27152-27168.

[16] Osamu Miyatake, Yasushi Koito, Kotaro Tagawa, Yasuhiro Maruta, Transient characteristics and performance of a novel desalination system based on heat storage and spray flashing, In Desalination, Volume 137, Issues 1–3, 2001, Pages 157-166, ISSN 0011-9164

[17] Faisal Al-Juwayhel, Hisham El-Dessouky, Hisham Ettouney, Analysis of single-effect evaporator desalination systems combined with vapor compression heat pumps, In Desalination, Volume 114, Issue 3, 1997, Pages 253-275, ISSN 0011-9164

[18] Sami Mutair, Yasuyuki Ikegami, Experimental investigation on the characteristics of flash evaporation from superheated water jets for desalination, In Desalination, Volume 251, Issues 1–3, 2010, Pages 103-111, ISSN 0011-9164.

[19] Hamawand, I., Lewis, L., Ghaffour, N., & Bundschuh, J. (2017). Desalination of salty water using vacuum spray dryer driven by solar energy. Desalination, 404, 182-191. doi: 10.1016/j.desal.2016.11.015.

[20] Gao, Wenzhong, et al. "An experimental investigation of salt-water separation in the vacuum flashing assisted with heat pipes and solid adsorption." Desalination 399 (2016): 116-123.

[21] Shusser M, Weihs D. Explosive boiling of a liquid droplet[J]. International journal of multiphase flow, 1999, 25(8): 1561-1573.

[22] Frost D L. Dynamics of explosive boiling of a droplet[J]. The Physics of fluids, 1988, 31(9): 2554-2561.

[23] Shusser M, Ytrehus T, Weihs D. Kinetic theory analysis of explosive boiling of a liquid droplet[J]. Fluid

Dynamics Research, 2000, 27(6): 353-365.

[24] Kelly R, Miotello A. Comments on explosive mechanisms of laser sputtering[J]. Applied Surface Science, 1996, 96: 205-215.

[25] Chen J K, Beraun J E. Modelling of ultrashort laser ablation of gold films in vacuum[J]. Journal of Optics A: Pure and Applied Optics, 2003, 5(3): 168.

[26] Owen, I., and J. M. Jalil. "Heterogeneous flashing in water drops." *International journal of multiphase flow* 17.5 (1991): 653-660.

[27] Liu, L., Q. C. Bi, and G. X. Wang. "Dynamics of evaporation and cooling of a water droplet during the early stage of depressurization." *Proceedings of the ASME International Mechanical Engineering Congress & Exposition, IMECE*. Vol. 12154. 2009.

[28] Gui Lu, Xiao-Dong Wang, Wei-Mon Yan, Nucleate boiling inside small evaporating droplets: An experimental and numerical study, In International Journal of Heat and Mass Transfer, Volume 108, Part B, 2017, Pages 2253-2261, ISSN 0017-9310

[29] R.S. Volkov, P.A. Strizhak.Research of temperature fields and convection velocities in evaporating water droplets using Planar Laser-Induced Fluorescence and Particle Image Velocimetry.Experimental Thermal and Fluid Science97(2018):392-407.

[30] R.S. Volkov, P.A. Strizhak, S.Y. Misyura, S.I. Lezhnin, V.S. Morozov.The influence of key factors on the heat and mass transfer of a sessile droplet.Experimental Thermal and Fluid Science99(2018):59-70.

[31] Nayar, Kishor G., Mostafa H. Sharqawy, and Leonardo D. Banchik. "Thermophysical properties of seawater: a review and new correlations that include pressure dependence." *Desalination*390 (2016): 1-24.

[32] Sharqawy, Mostafa H., John H. Lienhard, and Syed M. Zubair. "Thermophysical properties of seawater: a review of existing correlations and data." *Desalination and Water Treatment* 16.1-3 (2010): 354-380.

[33] P.A Strizhak,R.S. Volkov, S.Y. Misyura,S.I. Lezhnin,V.S. Morozov.The role of convection in gas and liquid phases at droplet evaporation.International Journal of Thermal Sciences,2018,Volume 134,pages 421-439.

[34] C.-H. Chun, Wuest, A micro-gravity simulation of the Marangoni convection, In Acta Astronautica, Volume 5, Issue 9, 1978, Pages 681-686, ISSN 0094-5765

[35] Ford J D, Missen R W. On the conditions for stability of falling films subject to surface tension disturbances; the condensation of binary vapors[J]. The Canadian Journal of Chemical Engineering, 1968, 46(5): 309-312.

[36] P.A. Pavlov, Evaporation of a highly superheated liquid, In International Journal of Heat and Mass Transfer,

Volume 88, 2015, Pages 203-209, ISSN 0017-9310

List of figure caption

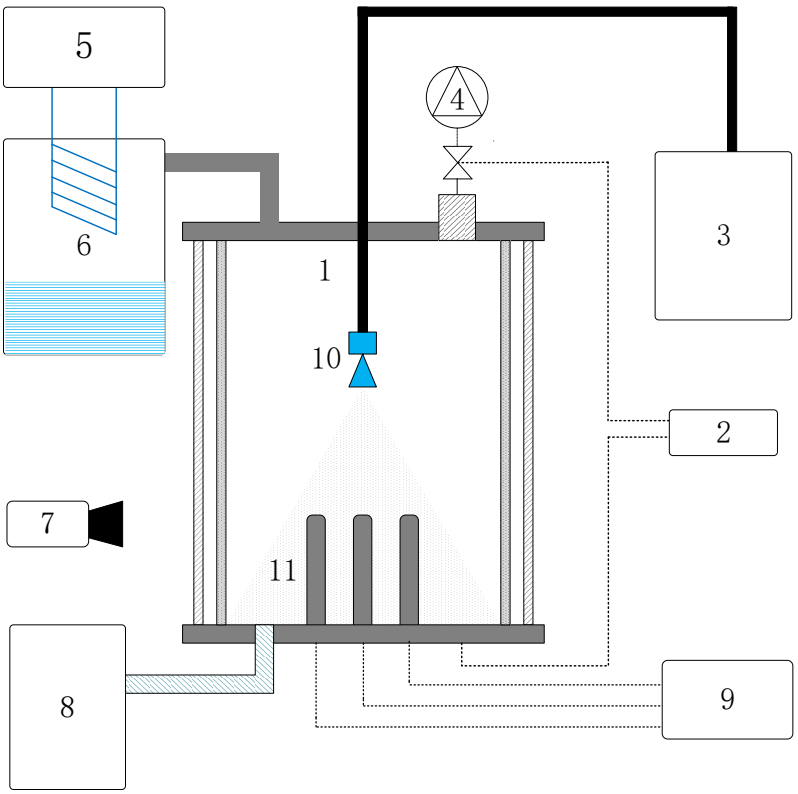

1.Flash chamber 2. Data logger 3. Dilute solution tank 4. Vacuum pump

5.Condenser 6. Condensing chamber 7. High speed camera

8. Concentrated solution tank 9. DC power supply

10. Centrifugal nozzle 11. Electric heating rod

Fig. 1 Experimental setup of device

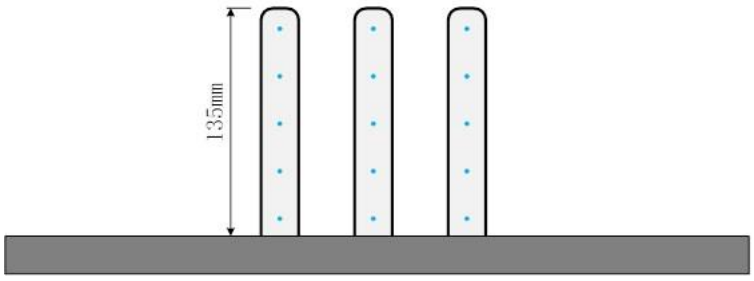

Fig. 2 Thermocouple distribution

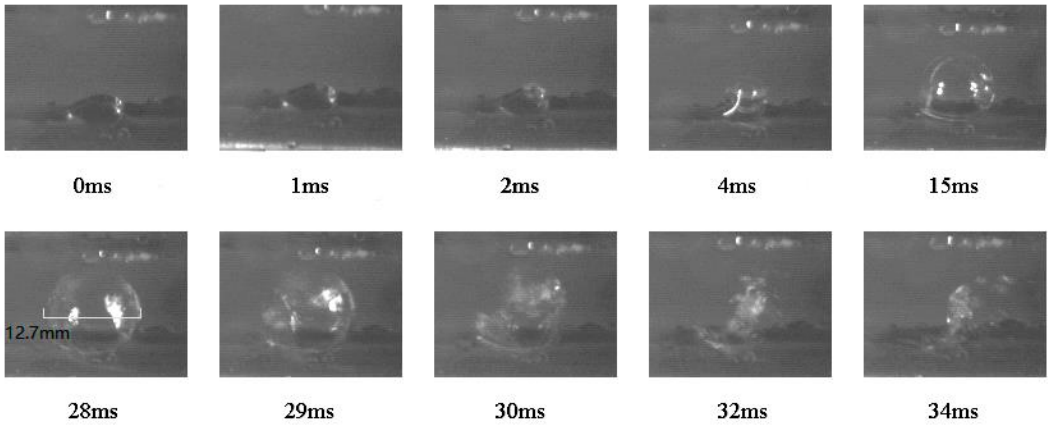

Fig. 3 Bubble fragmentation process of pure water

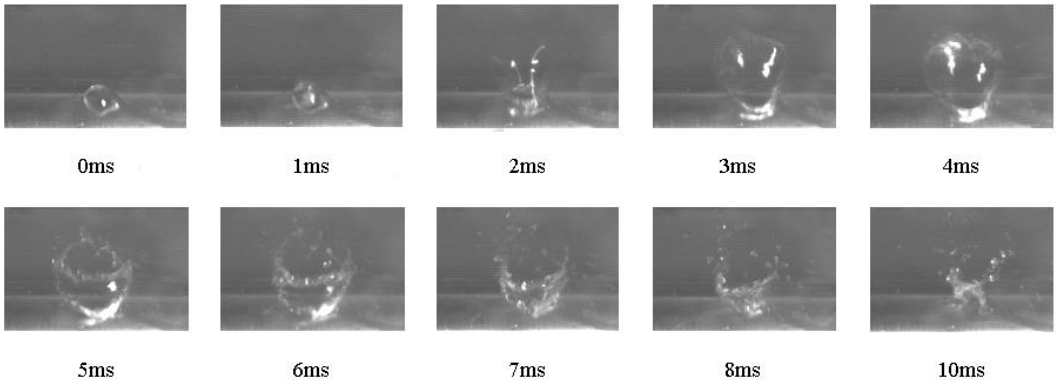

Fig. 4 Crown fragmentation process of pure water

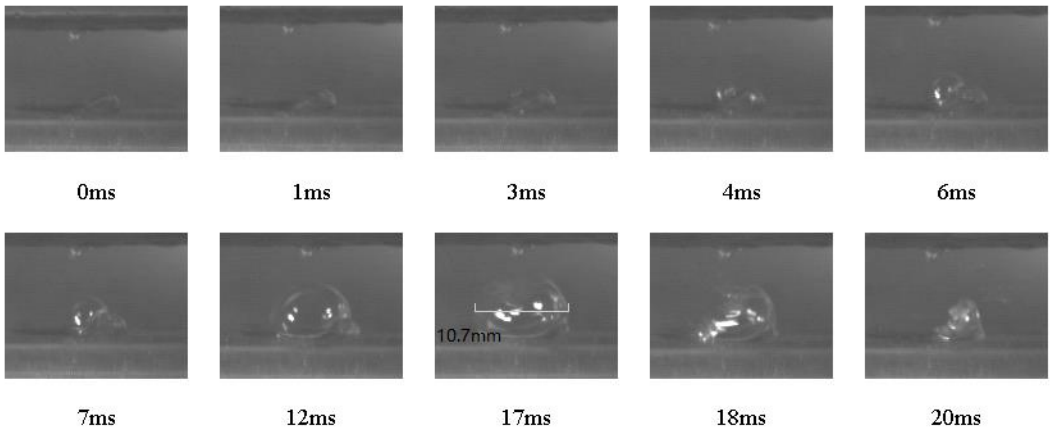

Fig. 5 Bubble fragmentation process of 3.5wt% salty water

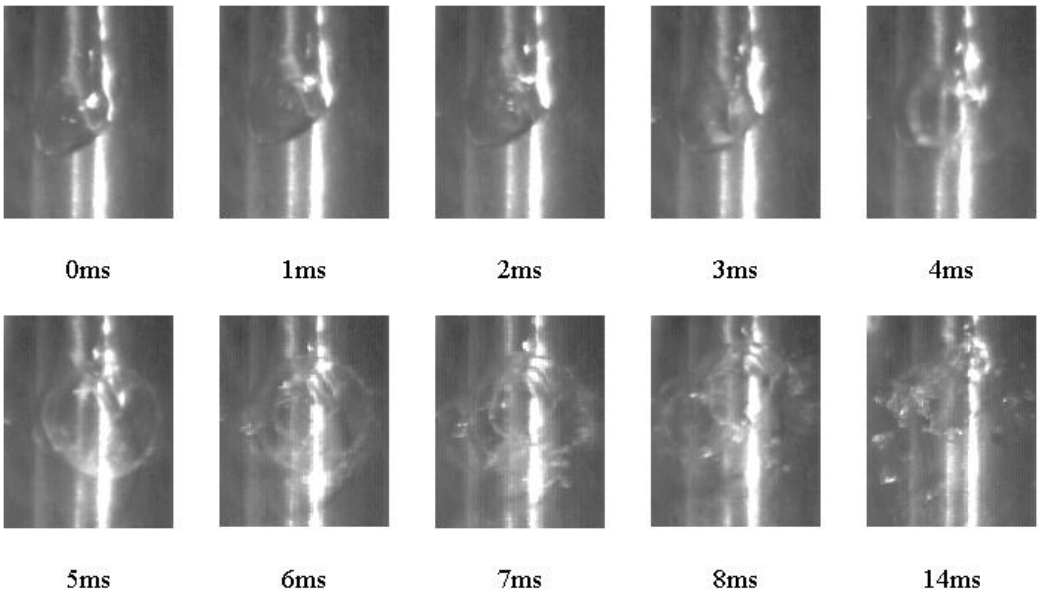

476

477 Fig. 6 Crown fragmentation process of 3.5wt% salty water

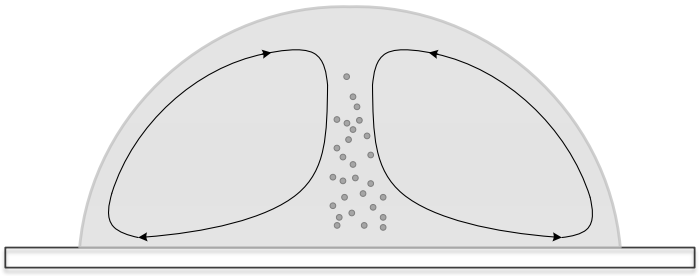

478

479 Fig. 7 Marangoni convection inside the droplets

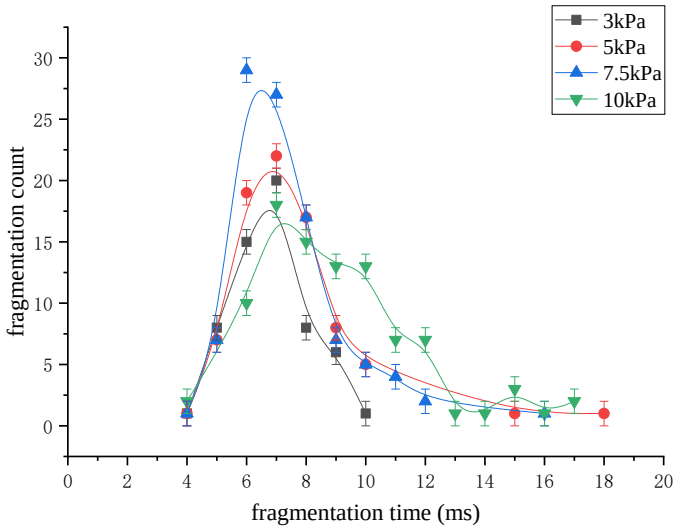

480

481 Fig. 8 Fragmentation time of pure water with different pressure

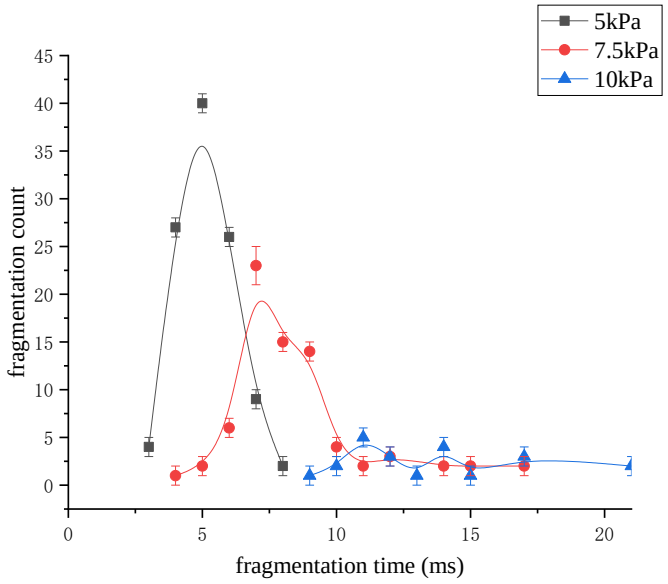

482

483 Fig. 9 Fragmentation time of 3.5wt% salty water with different pressure

484

485

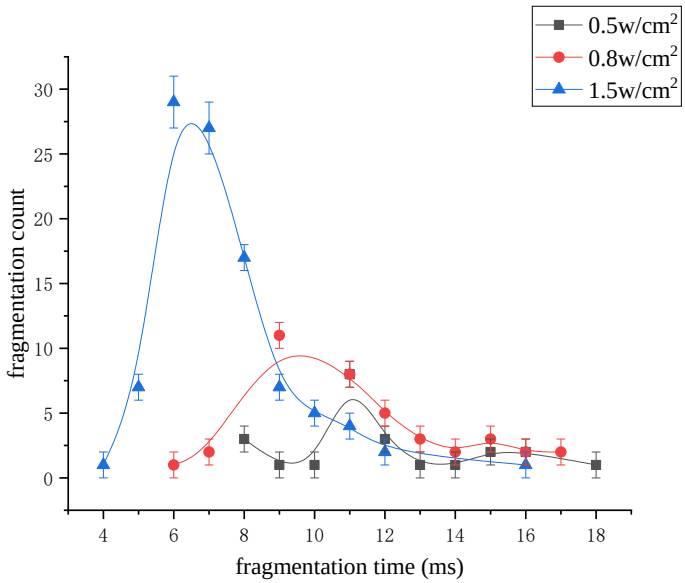

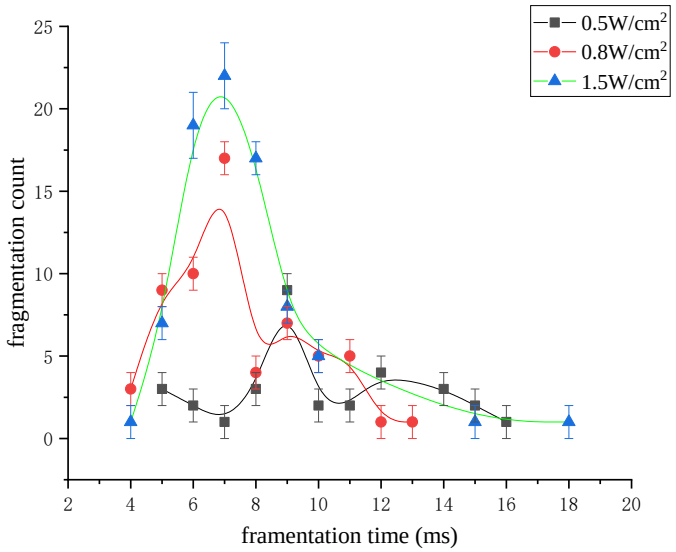

Fig. 10 Fragmentation time of pure water with different heat flux at the pressure of 5 kpa

Fig. 11 Fragmentation time of pure water with different heat flux at the pressure of 7.5 kpa

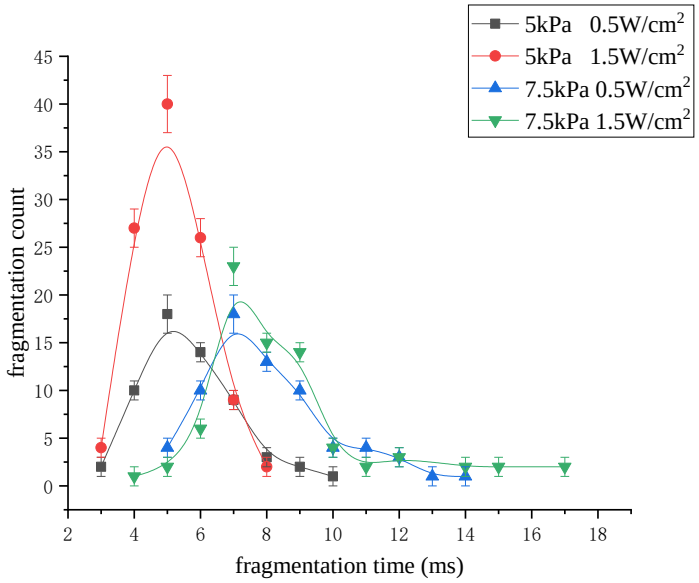

490

491 Fig. 12 Fragmentation time of 3.5wt% salty water with different heat flux at the pressure of 5 kpa, 7.5 kpa

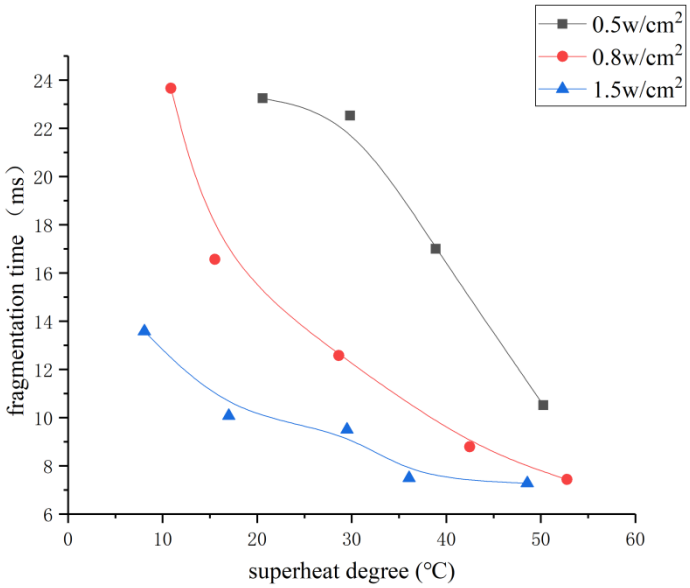

492 Fig. 13 Fragmentation time curve of pure water at the pressure of 5 kpa

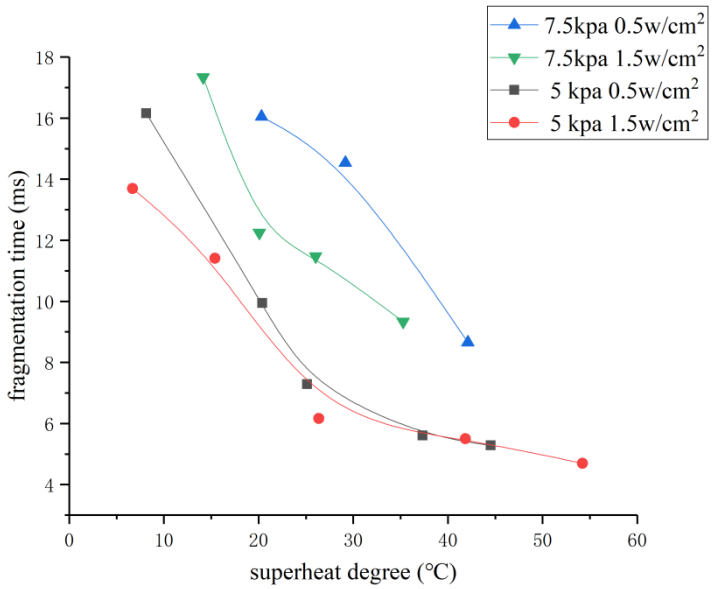

493

494 Fig. 14 Fragmentation time curve of 3.5wt% salty water at the pressure of 5 kpa, 7.5 kpa

495

496 Table 1 Performance index of test equipment

Test equipment	Unit	Range	Error
Agilent 34970A	/	/	2%±0.6% （23℃±1℃ at room temperature）
Omega thermocouple TT-T-36-SLE	℃	200~260	0.4% or 0.5℃ （the larger value shall prevail）
Pressure sensor	kPa	0-30	0.5%
Voltage of DC power	V	0-30	0.5%
Current of DC power	A	0-60	0.5%

497

498

499

500

501

Table 2 Testing conditions

Condition	Ambient pressure（kPa）	Surface temperature (℃)	Heat flux (w/cm^2)	Working fluid
1	5	40	0.5	water
2	5	80	1.5	water
3	5	40	0.5	seawater
4	5	50	1.5	seawater
5	3-10	80	0.5	water
6	3-10	80	0.5	seawater
7	5	80	0.5,0.8,1.5	water
8	5	80	0.5,0.8,1.5	seawater
9	7.5	80	0.5,0.8,1.5	water
10	7.5	80	0.5,0.8,1.5	seawater
11	5	40-80	0.5,0.8,1.5	water
12	5	40-80	0.5,0.8,1.5	seawater
13	7.5	40-80	0.5,0.8,1.5	water
14	7.5	40-80	0.5,0.8,1.5	seawater